This is an *Accepted Manuscript*, which has been through the Royal Society of Chemistry peer review process and has been accepted for publication.

Accepted Manuscripts are published online shortly after acceptance, before technical editing, formatting and proof reading. Using this free service, authors can make their results available to the community, in citable form, before we publish the edited article. We will replace this *Accepted Manuscript* with the edited and formatted *Advance Article* as soon as it is available.

You can find more information about *Accepted Manuscripts* in the **Information for Authors**.

Please note that technical editing may introduce minor changes to the text and/or graphics, which may alter content. The journal's standard **Terms & Conditions** and the **Ethical guidelines** still apply. In no event shall the Royal Society of Chemistry be held responsible for any errors or omissions in this *Accepted Manuscript* or any consequences arising from the use of any information it contains.

ARTICLE TYPE

1,8-Naphthyridine-based fluorescent receptors for picric acid detection in aqueous media

**Mandeep K. Chahal and Muniappan Sankar***

We utilized the potential applications of 1,8-naphthyridine based sensors for the detection of various nitroaromatics such as picric acid (PA), 3-nitrophenol (NP), 2,4-dinitrotoluene (DNT), 1,3-dinitrobenzene (DNB), 4-nitrotoluene (NT), nitrobenzene (NB) and nitromethane (NM). Among the various nitroaromatic analogues, nap-OH (**1**) and nap-Cl (**2**) sense picric acid (PA) much more efficiently, owing
10 to favourable electron and/or energy transfer mechanisms along with potential electrostatic interactions with very low detection limits (1.12 and 0.96 ppm). Interestingly, both sensors **1** and **2** detect PA in aqueous media (H_2O/CH_3OH, 8:2) with same quenching efficiency as in neat CH_3OH resulting in cheap, sensitive and environmental friendly detection methodology. Hence, minute molecules for picric acid detection in aqueous and methanolic solutions, having low detection limit along with exceptional
15 quenching constant (k_{SV}) overlaps with the present desires. In addition, sensors **1** and **2** exhibit instant visualization of trace amount of PA both in solid-state and using test strips.

The indiscriminate use of highly explosive substances such as nitroaromatics on a persistent basis is not only threatening the environment but is also challenging the overall security which
20 has left people edgy.[1] As a wise measure, the detection of such explosives requires immediate and effective consideration due to their antiterrorism applications. A wide variety of methods have been devised which can detect the presence of these explosives to varying degrees like trained canine teams,[2a] gas chromatography
25 coupled with mass spectrometry,[2b] gas chromatography-electron capture detection,[2c] surface-enhanced Raman spectroscopy,[2d] mass spectrometry,[3] X-ray imaging,[4a] thermal neutron analysis,[4b] electrochemical procedures[4c] and ion mobility spectroscopy (IMS).[5] Most of the current techniques known are either very
30 complex to carry out or are not cost effective which limits their widespread applicability. Thus, there is an urgent need to find an efficient and more reliable detection technique which is cheap and easy to implement. Among various transduction methods, the fluorescence technique is considered to be a most effective tool
35 for sensing nitro explosives owing to its simplicity, sensitivity, safety, cost effectiveness and short response time and the ability to be applied in both solution and solid state.[6]

In the last few years several fluorescent polymers,[7] MOFs,[8] quantum dots (QDs)[9] and small molecule-based sensors[10] have
40 been developed for the detection of nitroaromatics. Surprisingly very little attention has been given to sensitive detection of picric acid, although it has been shown to be a high-power explosive and is mainly used in the ammunition and explosive industry.[11] Apart from that, the explosive and poisonous nature of picric acid
45 renders its presence in the environment highly lethal. PA causes several health problems including damage to respiratory organs, skin irritation, nausea, skin allergy, vomiting, diarrhoea and cumulative liver, kidney and red blood cell damage.[12] In addition

to these detrimental effects, PA has also been recognized as a
50 toxic pollutant along with mutagenic properties.[13] Its strong UV-Vis absorption but poor fluorescence intensity makes its detection highly impractical. Furthermore, it is widely used in many pharmaceutical and dye industries, chemical laboratories and for the manufacturing of rocket fuels, fireworks and so on.[14] Owing
55 to its widespread uses, its presence in ground water and other drinking water sources can thus be explicitly catastrophic and an abomination for the general public. This makes the sensing of picric acid extremely important both for national security as well as for environmental safety.

60 In an independent approach, the introduction of small molecules[15] into the arena of picric acid detection has added a new dimension to the existing methods and has simultaneously brought a new hope in terms of pressure on the pockets at organizational and individual levels. The development of sensors
65 that can detect PA in aqueous media is the main focus of scientific community worldwide. The first 'small molecule based colorimetric and fluorescent receptor for PA detection' was reported in 2011.[16] Later, Kumar, Zheng, Mukherjee and others have published 'small molecules base sensors' for the detection
70 of PA.[17] Herein, we report a small molecule i.e. 1,8-naphthyridine based fluorescent sensors for the detection of PA both in neat CH_3OH and aq. methanolic solutions. **1** and **2** are easily adsorbed on hand held test strips. These test strips provide an easy way to detect trace amounts of PA without any experimental setup.

75
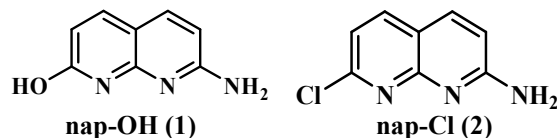
Fig. 1 Molecular structures of sensors **1** and **2**.

Experimental section

Materials and methods

All the chemicals used in this work were purchased from commercial sources and used without further purification. Solvents were dried and freshly distilled according to standard procedures. The receptors **1** and **2** were synthesized using reported literature methods.[18] UV-Visible spectra were recorded on an Agilent Cary 100 spectrophotometer, using a pair of quartz cells of 10 mm path length. The fluorescence spectra were recorded on a Hitachi F-4600 spectrofluorometer using a quartz cell of 10 mm path length. ^1H and ^{13}C NMR spectra were recorded on a Bruker AVANCE 500 MHz spectrometer in CDCl$_3$ and DMSO-d$_6$. HRMS-ESI mass spectra were recorded on a Bruker Daltanics micro-TOF mass spectrometer using CH$_3$CN as solvent. Fluorescence lifetime measurements were recorded on a Horiba Jobin Yvon 'FluoroCube Fluorescene Lifetime System'. The relative fluorescence quantum yields (φ) were estimated by using equation 1 by using the integrated emission intensity of anthracene (φ$_{fr}$ = 0.36 in cyclohexane) as a reference.

$$\phi_{fs} = \phi_{fr} (I_{sample}/I_{std})(A_{std}/A_{sample})(\eta^2_{sample} / \eta^2_{std}) \qquad \text{Eq. 1}$$

Where, φ$_{fr}$ is the absolute quantum yield for the anthracene used as reference; I$_{sample}$ and I$_{std}$ are the integrated emission intensities; A$_{sample}$ and A$_{std}$ are the absorbance at the excitation wavelength, and η$_{sample}$ and η$_{std}$ are the refractive indices.

Sensors **1** and **2** were synthesised using one step reported procedure.[18]

2-amino-7-hydroxy-1,8-napthyridine (nap-OH (1)): ^1H NMR (500 MHz, DMSO-d$_6$) δ$_H$ 11.51 (1H, br s, OH), 7.67 (2H, m, 2 × CH), 6.75 (2H, br s, NH$_2$), 6.37 (1H, d, J = 8.5 Hz, CH), 6.14 (1H, d, J = 9.5 Hz, CH); ^{13}C NMR (125 MHz, DMSO-d$_6$) δ$_C$ 163.7, 160.5, 150.4, 139.7, 137.3, 114.8, 105.2, 104.9. HRMS (ESI+) [M+H]$^+$ calcd. 162.058, found 162.059.

2-amino-7-chloro-1,8-napthyridine (nap-Cl (2)): ^1H NMR (500 MHz, DMSO-d$_6$) δ$_H$ 7.86 (2H, m, 2 × CH), 7.18 (1H, d, J = 8.4 Hz), 6.77 (1H, d, J = 8.8 Hz), 5.28 (bs, 2H); ^{13}C NMR (125 MHz, DMSO-d$_6$) δ$_C$ 161.4, 139.5, 137.4, 117.1, 115.7, 113.5, 79.1. HRMS (ESI+) [M+H]$^+$ calcd. 180.032, found 180.030.

Fluorescence titrations

Fluorescence titrations were performed using freshly prepared 40 μM solutions of **1** and **2** in CH$_3$OH and H$_2$O:CH$_3$OH (8:2, v/v). To these, aliquots of freshly prepared stock solution (2×10^{-3} M) of nitroaromatic compounds (NACs) were added. The titration experiments were performed at 298 K and each titration was repeated three times to the get concordant outcomes. For all measurements, **1** and **2** were excited at λ$_{ex}$ = 340 and 345 nm, respectively.

Computational Methodology

Full geometry optimizations were carried out using Gaussian 09 package.[19] The hybrid B3LYP functional has been used in all calculations as implemented in Gaussian 09 package, mixing the exact Hartree-Fock-type exchange with Becke's expression for the exchange functional[20] and that proposed by Lee-Yang-Parr for the correlation contribution.[21] The 6-311+G(d,p) basis set was used for all calculations. Frequency calculations carried out on the optimized structures confirmed the absence of any imaginary frequencies.

Results and discussion

The fluorophores (**1** and **2**) were synthesized[18] in quantitative yields by reported methods. They were fully characterized by various spectroscopic methods such as UV-Visible, fluorescence and multinuclear NMR (^1H and ^{13}C) and electrospray ionization mass spectrometry (ESI-MS) (Figures S1-S6, ESI). The fluorescence spectra of **1** and **2** in CH$_3$OH exhibit strong emission at 385 and 397 nm when excited at 340 and 345 nm, respectively (Figure S7 in the ESI). The emissive nature of **1** (Φ = 0.72) and **2** (Φ = 0.32) encouraged us to investigate their potential use for the detection of nitroaromatics.

To explore the ability of **1** and **2** to detect trace quantities of nitro explosives, fluorescence titrations were performed with the incremental addition of analytes. Fast and effective fluorescence quenching was observed only upon incremental addition of PA solution. Upon addition of 4.5 equiv and 4 equiv of picric acid, the emission bands of **1** and **2** were completely quenched (Figures 2a and 2b). The Stern-Volmer (SV) plots were linear at low concentrations and subsequently deviated from linearity, bending upwards at higher concentrations of PA (Figures S8-S9 in ESI). The nonlinear nature of the SV plot can be ascribed to self-absorption, a combination of both static and dynamic quenching and an energy transfer process between PA and receptors.[22]
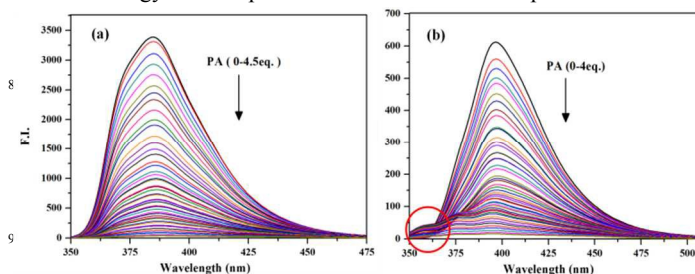

Fig. 2 (a) Change in fluorescence intensity of **1** (40 μM) upon addition of **PA** (0 - 18 × 10^{-5} M); (b) Change in fluorescence intensity of **2** (40 μM) with the incremental addition of **PA** (0 - 16 × 10^{-5} M) in CH$_3$OH.

Therefore, we applied an exponential quenching equation I$_0$/I = Ae$^{k[Q]}$ + B.[23] Nonlinear SV curves fitted to the exponential equations of I$_0$/I = 2.423e$^{20602.68[PA]}$–1.944 and I$_0$/I = 2.237e$^{18277.26[PA]}$–1.628 for **1** and **2**, respectively. A linear Stern-Volmer plot was obtained from fluorescence titration at low concentration of PA (64 μM) for the sensor **1** having k_{SV} of 7.203 × 10^4 M^{-1}. Similarly, for sensor **2**, the Stern-Volmer plot was linear till 32 μM concentration of PA with quenching constant of 3.903 × 10^4 M^{-1}. In depth analysis of fluorescence titration profiles lead us to conclude that both sensors interact differently with PA. Furthermore, the fluorescence quenching titrations were also performed with other nitroaromatics such as 3-nitrophenol (NP), 2,4-dinitrotoluene (DNT), 1,3-dinitrobenzene (DNB), 4-nitrotoluene (NT), nitrobenzene (NB) and nitromethane (NM). All other nitro compounds showed little effect on the fluorescence intensity (Figures S10-S11 in ESI). The quenching of fluorescence intensity of **1** in CH$_3$OH was observed with excess of NP (>20 equiv.), DNT (> 88 equiv.), NT (> 128 equiv.), DNB (>144 equiv.), NB (> 176 equiv.) and NM (>576

equiv.) (Fig. S12 in the ESI). Also, the quenching of fluorescence emission of **2** in CH$_3$OH was observed with excess NP (> 22 equiv.), DNT (> 96 equiv.), NT (> 256 equiv.), DNB (> 240 equiv.), NB (> 288 equiv.) and NM (> 480 equiv.) (Fig. S13 in the ESI). However, in case of picric acid complete fluorescence quenching of **1** and **2** (40 μM) was observed for much lower concentrations viz. 180 μM (4.5 equiv. for **1**) and 160 μM (4 equiv. for **2**).
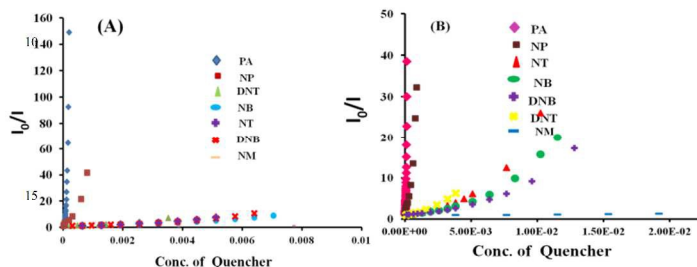

Fig. 3 The Stern-Volmer plots for different concentration of various nitroaromatics for sensor **1** (A) and for sensor **2** (B) in CH$_3$OH.

This clearly demonstrates the high selectivity of **1** and **2** towards PA over other nitro analytes. From the SV plots in CH$_3$OH, we were able to calculate the quenching constants and analyse the quenching efficiencies of various analytes (Figure 3).[23] Table 1 lists the SV quenching constants and detection limits data of sensors **1** and **2**. These sensors are highly sensitive and can detect PA down to 1.12 and 0.96 ppm, respectively (figures S14 and S15, ESI). We also investigated to see if protonation of the sensors was the conclusive factor behind the fluorescence quenching of the sensors **1** and **2**. In this regard, the fluorescence spectra of the sensors were recorded in the presence of excess trifluoroacetic acid (TFA) (which is slightly more acidic than PA), which showed a negligible effect on the fluorescence intensity of the sensors compared to PA (Figs. S16a and S17b, ESI). The quenching efficiencies remain almost same for PA under both acidic and basic conditions (Figs. S16b and S17b). Also, the response of sensors was same for PA even in the presence of excess of TFA (Figs S16c and S17c).

Table 1. The SV quenching constants and detections limits data of sensors **1** and **2** in CH$_3$OH at 298 K.

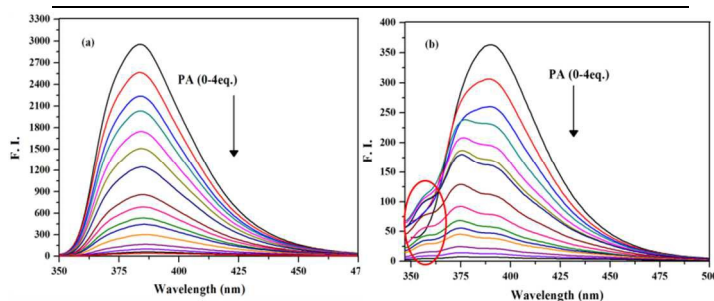| Sensor	Stern-Volmer Constant (k_{SV}) (M^{-1})	Detection Limit (ppm)
1	7.203×10^4	1.12 (4.89 μM)
2	3.903×10^4	0.96 (4.16 μM)

Fig. 4 Fluorescence spectra of the sensor **1** (a) and sensor **2** (b) (40μM) upon addition of PA in H$_2$O/CH$_3$OH (8:2, v/v).

Sensing Studies in Aqueous Media

In order to explore the empirical utilizability of these molecules, the spectral response of the synthesized moieties was investigated in aqueous medium (H$_2$O:CH$_3$OH, 8:2, v/v). Aqueous medium was chosen because it is the solvent which nature utilizes to sustain life. The quenching efficiencies of these sensors are found to be similar in neat methanol and aqueous methanol (H$_2$O:CH$_3$OH, 8:2, v/v), providing that these sensors can detect PA in aqueous solutions. The ideal experimental results obtained herein demonstrated the practical applicability of the sensors toward PA sensing. Interference experiments to determine the effects of other nitroaromatics on the interaction of PA with both the sensors were also conducted (Figures S18-S19, ESI); the fluorescence emission intensity of sensors **1** and **2** was almost unaffected.

Lifetime studies

To get more insight into the sensing mechanism, time-resolved decays were measured in the presence of PA. The decay profile of nap-OH (**1**) and nap-Cl (**2**) upon titration of PA are illustrated in Figures S20-S21 in the ESI, which shows that fluorescence lifetime is found to be invariant at different concentrations of PA. The Stern−Volmer plots for **1** and **2** are illustrated in (Figures 5a and 5b) the forms of both I$_0$/I and τ$_0$/τ, where I$_0$ and I are the steady-state fluorescence intensity in absence and presence of the quencher and τ$_0$ and τ are the fluorescence lifetime in absence and presence of the quencher, respectively.
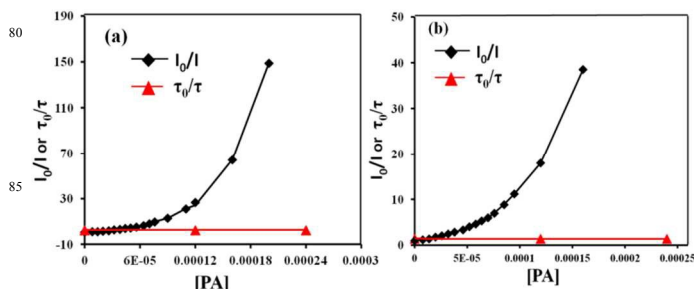

Fig. 5 Fluorescence quenching plots of intensity ratio (I$_0$/I) and lifetime ratio (τ$_0$/τ) of (a) sensor **1** (b) sensor **2** solution to the concentration of target explosives.

Figure 5 suggests that the quenching is static in nature and a ground state complex is formed between the sensors (**1** and **2**) and PA. These results implied that there are strong interactions between the sensors (**1** and **2**) and PA. The UV-Vis absorption of the fluorophores upon addition of PA was also measured. As seen in Figures S22 and S23 in the ESI, PA, nap-OH (**1**) and nap-Cl (**2**) have their own absorption which is very strong and makes it hard to observe obvious variation in absorption bands upon addition of PA. Fluorescence responses of the fluorophores were also measured at various excitation wavelengths (340, 345, 350 and 360 nm) to check the influence from PA absorption. It was found that by varying the excitation wavelength caused no significant change in quenching efficiencies (Figures S24 and S25 in ESI), indicating that absorption of PA does not contribute to the observed fluorescence quenching.[24]

Fluorescence Quenching Mechanism

To understand the origin of the high selectivity of **1** and **2**

towards PA, the mechanism of quenching was explored. Figures 6 and S26 in the ESI show the HOMO and LUMO orbital energies of electron deficient nitro compounds in gas phase and methanol, respectively. The LUMO energies were in good agreement with the maximum quenching observed for PA[25a-b], but the order of observed quenching efficiency is not fully in accordance with the LUMO energies of other nitroaromatics.[10c,22a,25b-c] For other NACs, quenching efficiencies follow the order: DNB > DNT > NP > NB > NT > NM. This indicates that the photoinduced electron transfer (PET) is not the only mechanism for quenching.
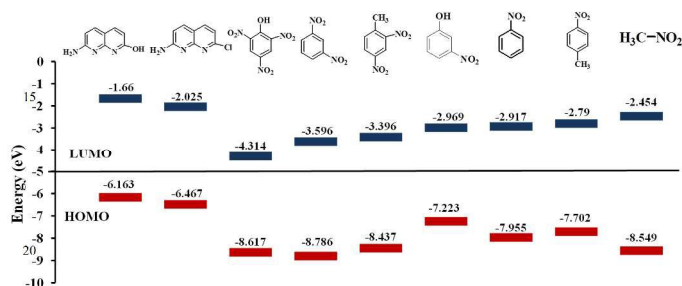

Fig. 6 HOMO and LUMO energies of the frontier orbitals of the fluorophores, quencher and other electronegative analytes in the gas phase.

The non-linear SV plot for PA suggests an energy transfer mechanism. The resonance energy transfer can occur from a fluorophore to a non-emissive analyte, if the fluorophore and analyte are close to each other and the absorption band of the analyte has an effective overlap with the emission band of the fluorophore. Förster resonance energy transfer (FRET) can dramatically enhance the fluorescence quenching efficiency and also improve the sensitivity.[26]
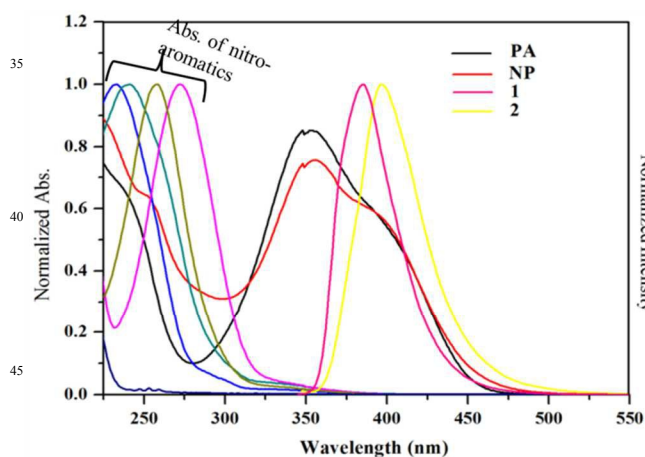

Fig. 7 Spectral overlap between the absorption spectra of analytes and the emission spectra of sensors **1** and **2**.

Figure 7 shows that the absorption spectrum of PA and NP has a large overlap with the emission spectrum of **1** and **2**, whereas almost no overlap was observed for DNT, DNB, NT, NB and NM. This result suggests that the main quenching mechanism for PA is the energy transfer.[26] For other nitro compounds, the quenching occurs only by electron transfer. The energy transfer is a long range process, thus emission quenching by PA is carried over to the surrounding fluorophores, thereby amplifying the

quenching response of **1** and **2**. On the other hand, electron transfer is a short range process, so that emission quenching by other nitro compounds is limited to the fluorophores that have direct interaction with the analytes. Thus, **1** and **2** respond more selectively to PA than to other nitroaromatic compounds.

The quenching efficiency was high for the electron deficient NACs having acidic –OH group. So, the presence of electrostatic interactions can lead to the special selectivity of **1** and **2** for PA. The fluorescence quenching titrations were also performed with 4-nitrophenol (NP). The order of the quenching efficiency was found to be PA > NP, which is in complete agreement with the order of acidity of these analytes (PA > NP). This may explain the unprecedented selectivity for PA, as other nitro compounds do not have a hydroxyl group and hence cannot interact strongly with the free basic sites of the fluorophores (free amine nitrogen and naphthyridine nitrogen on the surface) and so result in a very low quenching. On the other hand, hydroxyl group containing analytes such as PA, NP can interact with the basic sites of **1** and **2**, and do so in the order of their acidity. PA, with its highly acidic hydroxyl group interacts strongly with the fluorophores and the quenching effect is carried over long range owing to the energy transfer mechanism, thus leading to an amplified response. As compared to other nitro compounds, sensors **1** and **2** exhibit a much higher fluorescence quenching response towards PA, owing to favourable electron and energy transfer mechanisms, as well as electrostatic interactions. Thus, the presence of free basic sites in sensors **1** and **2** can be a useful tool to achieve the selective detection of PA over other nitro compounds.

Mode of binding of 1 and 2

Sensor **1**, 2-amino-7-hydroxy-1,8-naphthyridine tautomerises to the corresponding 2-amino-1,8-naphthyrid-7-one (figure S27, ESI).[27] As a result the aromatic nitrogen atoms of sensor **1** are not as electron rich as the aromatic nitrogen atoms of sensor **2**. The interaction between the sensors and PA in solution was further studied *via* ^{1}H NMR experiments (Figs. 8 and S28, ESI). The signals of the hydrogen atoms located on the aromatic rings generally shifted downfield upon addition of 2.0 equiv aliquots of PA. In case of sensor **1**, the difference in chemical shifts ($\Delta\delta$) was 0.187, 0.174 and 0.231 ppm, respectively. The chemical shifts ($\Delta\delta$) of sensor **2** were comparatively downfield shifted as compared to **1** (0.363, 0.4255, 0.4755 and 0.3035). These results suggest that the nitrogen atom of the naphthyridine ring moiety of **2** was the only reasonable site for possible hydrogen-bonded interaction with PA while in case of sensor **1** interaction with free amine group occurs readily.
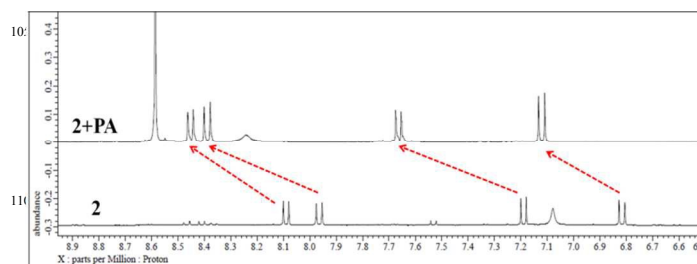

Fig. 8 ^{1}H NMR spectra (400 MHz) of the sensor **2** with PA in DMSO-d_6.

In Fig. 8, the peaks at 7.08 and 8.22 ppm correspond to -NH$_2$

before and after addition of picric acid. The shift of NH_2 protons from 7.08 to 8.22 ppm occurs possibly due to hydrogen bonding between NH_2 of **2** and OH of picric acid as shown in Figure 8. In case of sensor **2,** the chemical shifts for aromatic protons after addition of *m*-nitrophenol are in accordance with PA (Fig S29, ESI). Furthermore, we have carried out cyclic voltammetric studies for sensor **1**. **1** has exhibited an irreversible oxidation potential at 1.25 V (*vs.* Ag/AgCl reference electrode) due to oxidation of amine moiety (Fig. S30, ESI). In contrast, PA and other nitroaromatics exhibited anodic shift (positive) in redox potentials (Fig. 6) which indicate their facile reduction and electron accepting character. Particularly, phenolic nitroaromatics can easily accept an electron from sensors **1** and **2** to form donor-acceptor complexes.

Both **1** and **2** undergo fluorescence quenching on addition of PA but their mode of interaction is different. More insight into the fluorescence titration curves revealed that in case of sensor **1**, the fluorescence intensity quenches completely but in case of sensor **2** there is generation of a new band as shown by circle in figure 2(b). This fact is further supported by the optimized structure obtained for both **nap-OH (1)•PA** and **nap-Cl (2)•PA** *via* quantum chemical calculations using B3LYP/6-311+G(d,p) program (Figures 9 and 10). The DFT-optimized structures of both **1** and **2** with PA confirm their different modes of interaction supporting the results of fluorescence titration profiles. The optimized structure for **1•PA** shows proton transfer from the acidic –OH to –NH_2 group of **1** (formation of NH_3^+ on **1**) whereas the DFT-optimized structure for **2•PA** shows a dissimilar mode
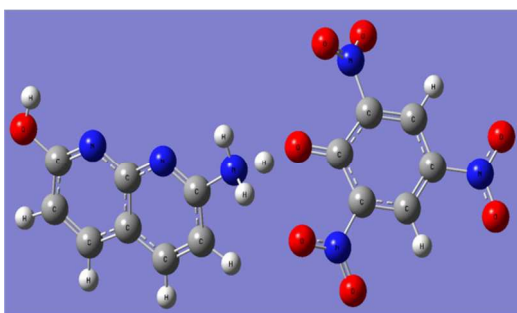

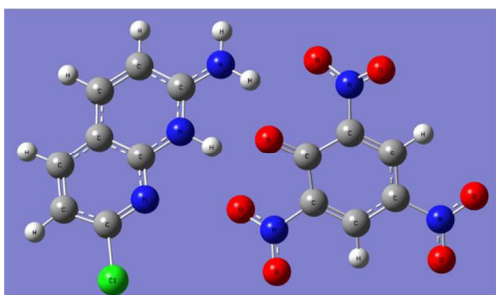**Fig. 9** B3LYP/6-311+G(d,p) optimized geometry of **1•PA** in gas phase.

Fig. 10 B3LYP/6-311+G(d,p) optimized geometry of **2•PA** in gas phase.

of interaction. The nitrogen of the naphthyridine **group of 2 interacts with –OH group of PA**, resulting in change of naphthyridine group from a hydrogen-bond acceptor to a hydrogen-bond donor (Fig. 10 and 11). Hence, the binding event is likely to be based on the interaction between nitrogen and phenolic -OH group. To support this view we did the titration in

presence of both phenol and *o*-dichlorobenzene. Fluorescence quenching was observed only in the presence of large excess of phenol and both the sensors remain insensitive to electron-deficient *o*-dichlorobenzene (Figures S31-S32, ESI). As shown in Figures S33-S34, the results revealed that the energies of the highest occupied molecular orbital (HOMO) and lowest unoccupied molecular orbital (LUMO) of sensor **1** were -6.16eV and -1.66eV, respectively, while those of **1•PA** were -7.1eV and -3.3eV, respectively. Similarly for sensor **2**, HOMO and LUMO were -6.46eV and -2.02eV, respectively, while for **2•PA** energies were -6.73eV and -3.44eV. Meanwhile, the energies of **1•PA** and **2•PA** were minimal, which indicated that **1•PA** and **2•PA** are stable.
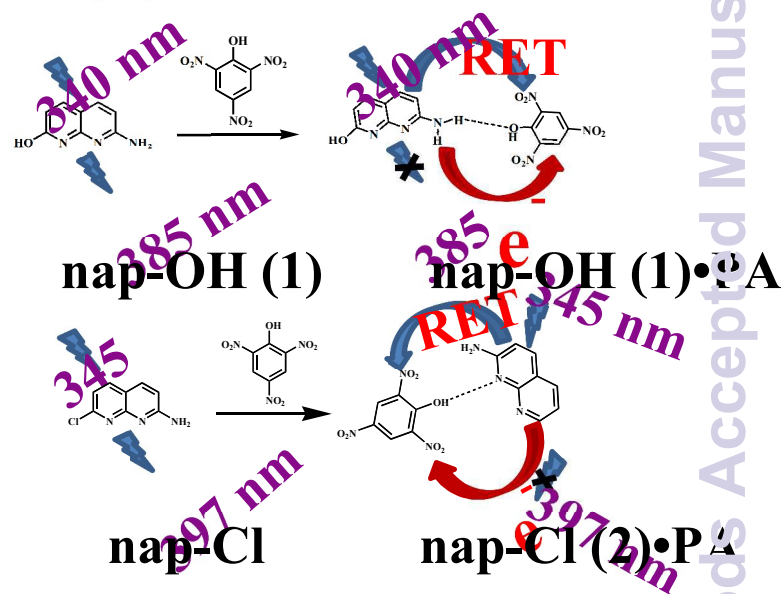
Summary of quenching mechanism

Fig. 11 Plausible scheme for picric acid sensing by sensors **1** and **2**.

Picric Acid Detection in Solid State and using Test Strips

Visual detection of trace amounts of picric acid is very convenient for security scanning and prompt identification. For this purpose, Compounds **1** and **2** were adsorbed on TLC plates showing strong emission which becomes non-emissive when spot of PA solution was co-adsorbed on these compounds (**Fig. 12**). We prepared the test-strips by dip-coating Whatman filter paper in CH_3OH solution of sensor **1** and **2** followed by drying in air.
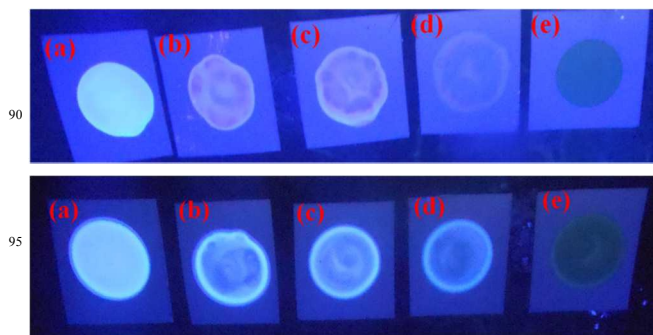

Fig. 12 Fluorescence image of (Upper) compound **1** (a) adsorbed on a TLC plate with a spot of PA solution (b) 10^{-5} M (c) 10^{-4} M (d) 10^{-3} M (e)

10^{-2} M. (Lower) compound **2** (a) adsorbed on a TLC plate with a spot of PA solution (b) 10^{-5} M (c) 10^{-4} M (d) 10^{-3} M (e) 10^{-2} M.

Then the strip was dipped into the methanolic solution of PA and as expected fluorescence quenching was observed after illuminating under UV lamp (Figure S35, ESI). This observation demonstrated the instant visualization of trace amounts of PA.

Conclusions

In conclusion, we are reporting 1,8-naphthyridine-based minute molecules for picric acid detection in neat methanol and aqueous methanolic solutions with very low detection limits. Among the various nitroaromatics, nap-OH (**1**) and nap-Cl (**2**) sense picric acid (PA) much more efficiently, owing to favourable electron and/or energy transfer mechanisms along with potential electrostatic interactions. The experimental results are in fair accordance with computational studies (DFT calculations) regarding the mechanism and mode of interaction. The results reported herein are a valuable addition to the field of small molecule-based sensors for highly explosive picric acid.

Notes and references

Mandeep K. Chahal and Muniappan Sankar*

Department of Chemistry, Indian Institute of Technology Roorkee, Roorkee - 2476667, Uttrakhand, India.

E-mail: *sankafcy@iitr.ac.in*; Tel: +91-1332-28-4753; Fax: +91-1332-27-3560.

†Electronic Supplementary Information (ESI) available: UV-Vis, FL and NMR spectra of **1** and **2**, UV-Vis and FL titrations of **1** and **2** for picric acid sensing, SV plots, DFT optimized structures and their frontier molecular orbitals (FMOs) of **1**, **2**, **1•PA** and **2•PA**. See DOI: 10.1039/b000000x/.

1   (a) Z. Hu, B. J. Deibert and J. Li, *Chem. Soc. Rev.,* 2014, **43,** 5815-5840; (b) Y. Salinas, R. Martínez-Máñez, M. D. Marcos, F. Sancenon, A. M. Costero, M. Parra and S. Gil, *Chem. Soc. Rev.,* 2012, **41,** 1261-1296.

2   (a) K. G. Furton and L. J. Myers, *Talanta,* 2001, **54,** 487-500; (b) K. Hakansson, R. V. Coorey, R. A. Zubarev, V. L. Talrose and P. Hakansson, *J. Mass Spectrom.,* 2000, **35,** 337-346; (c) M. E. Walsh, *Talanta,* 2001, **54,** 427-438; (d) J. M. Sylvia, J. A. Janni, J. D. Klein and K. M. Spencer, *Anal. Chem.,* 2000, **72,** 5834-5840.

3   (a) J. Yinon, *Mass Spectrom. Rev.,* 1982, **1,** 257-307; (b) J. C. Mathurin, T. Faye, A. Brunot and J. C. Tabet, *Anal. Chem.,* 2000, **72,** 5055-5062.

4   (a) S. F. Hallowell, *Talanta,* 2001, **54,** 447-458; (b) C. Vourvopoulos and P. C. Womble, *Talanta,* 2001, **54,** 459-468; (c) M. Krausa and K. Schorb, *J. Electroanal. Chem.,* 1999, **461,** 10-13.

5   (a) E. Wallis, T. M. Griffin, N. Popkie, Jr., M. A. Eagan, R. F. McAtee, D. Vrazel and J. McKinly, *Proc. SPIE-Int. Soc. Opt. Eng.,* 2005, **5795,** 54-64; (b) G. A. Eiceman and J. A. Stone, *Anal. Chem.,* 2004, **76,** 390A-397A.

6. (a) M. E. Germain and M. J. Knapp, *Chem. Soc. Rev.,* 2009, **38,** 2543-2555; (b) T. H. Liu, L. P. Ding, K. R. Zhao, W. L. Wang and Y. Fang, *J. Mater. Chem.,* 2012, **22,** 1069-1077; (c) S. J. Toal and W. C. Trogler, *J. Mater. Chem.,* 2006, **16,** 2871-2883.

7 (a) D. C. Apodaca, R. B. Pernites, F. R. D. Mundo and R. C. Advincula, *Langmuir,* 2011, **27,** 6768-6779; (b) A. Narayanan, O. P. Varnavski, T. M. Swager and T. Goodson, *Phys. Chem. C,* 2008, **112,** 881-884; (c) X. Wang, Y. Guo, D. Li, H. Chen and R.-c. Sun, *Chem. Commun.,* 2012, **48,** 5569-5571; (d) L. Feng, H. Li, Y. Qu and C. Lü, *Chem. Commun.,* 2012, **48,** 4633-4635; (e) B. Gole, W. Song, M. Lackinger and P. S. Mukherjee, *Chem. Eur. J.,* 2014, **20,** 13662-13680; (f) W. Wei, R. Lu, S. Tang and X. Liu, *J. Mater. Chem. A,* 2015, **3,** 4604-4611.

8 (a) S. S. Nagarkar, B. Joarder, A. K. Chaudhari, S. Mukherjee and S. K. Ghosh, *Angew. Chem. Int. Ed.,* 2013, **52,** 2881-2885; (b) X.-Z. Song , S.-Y. Song, S.-N. Zhao, Z.-M. Hao, M. Zhu, X. Meng, L.-L. Wu and H.-J. Zhang, *Adv. Funct. Mater.,* 2014, **24,** 4034-4041; (c) S. S. Nagarkar, A. V. Desai and S. K. Ghosh, *Chem. Commun.,* 2014, **50,** 8915-8918; (d) X.-H. Zhou, L. Li, H.-H. Li, A. Li, T. Yanga and W. Huang, *Dalton Trans.,* 2013, **42,** 12403-12409; (e) S.-R. Zhang, D.-Y. Du, J.-S. Qin, S.-J. Bao, S.-L. Li, W.-W. He, Y.-Q. Lan, P. Shen, and Z.-M. Su, *Chem. Eur. J.,* 2014, **20,** 3589-3594; (f) D. Tian, Y. Li, R.-Y. Chen, Z. Chang, G.-Y. Wang and X.-H. Bu, *J. Mater. Chem. A,* 2014, **2,** 1465-1470; (g) Y.-N. Gong, L. Jiang and T.-B. Lu, *Chem. Commun.,* 2013, **49,** 11113-11115; (h) L. Li, S. Zhang, L. Xu, L. Han, Z.-N. Chen and J. Luo, *Inorg. Chem.,* 2013, **52,** 12323-12325; (i) S. Sanda, S. Parshamoni, S. Biswas and S. Konar, *Chem. Commun.,* 2015, **51,** 6576-6579; (j) C. Zhang, L. Sun, Y. Yan, J. Li, X. Song, Y. Liu and Z. Liang, *Dalton Trans.,* 2015, **44,** 230-236; (k) A. Li, L. Li, Z. Lin, L. Song, Z.-H. Wang, Q. Chen, T. Yang, X.-H. Zhou, H.-P. Xiao and X.-J. Yin, *New J. Chem.,* 2015, **39,** 2289-2295.

9   B. Liu, C. Tong, L. Feng, C. Wang, Y. He and C. Lü, *Chem. Eur. J.,* 2014, **20,** 2132-2137.

10 (a) N. Venkatramaiah, S. Kumar and S. Patil, *Chem. Commun.,* 2012, **48,** 5007-5009; (b) Y. Zhao, W. Hao, W. Ma, Z. Zang, H. Zhang, X. Liu, S. Zou, H. Zhang, W. Liu and J. Gao, *New J. Chem.,* 2014, 38, 5754-5760; (c) P. Vishnoi, M. G. Walawalkar, S. Sen, A. Datta, G. N. Patwari and R. Murugavel, *Phys. Chem. Chem. Phys.,* 2014, **16,** 10651-10658; (d) T. Naddo, Y. Che, W. Zhang, K. Balakrishnan, X. Yang, M. Yen, J. Zhao, J. S. Moore and L. Zang, *J. Am. Chem. Soc.,* 2007, **129,** 6978-6979; (e) K. K. Kartha, S. S. Babu, S. Srinivasan, and A. Ajayaghosh, *J. Am. Chem. Soc.,* 2012, **134,** 4834-4841; (f) M. Wang, V. Vajpayee, S. Shanmugaraju, Y.-R. Zheng, Z. Zhao, H. Kim, P. S. Mukherjee, K. W. Chi and P. J. Stang, *Inorg. Chem.,* 2011, **50,** 1506-1512; (g) J.-F. Xiong, J.-X. Li, G.-Z. Mo, J.-P. Huo, J.-Y. Liu, X.-Y. Chen and Z.-Y. Wang, *J. Org. Chem.,* 2014, **79,** 11619-11630; (h) V. Beréau, C. Duhayon and J.-P. Sutter, *Chem. Commun.,* 2014, **50,** 12061-12064; (i) D. Udhayakumari, S. Velmathi, P. Venkatesan and S.-P. Wu, *Anal. Methods,* 2015, **7,** 1161-1166.

11 J. Akhavan, *Chemistry of Explosives,* Royal Society of Chemistry, London, 2nd edn, 2004.

12 Safety Data Sheet for Picric Acid, Resource of National Institute of Health; J. F. Wyman, M. P. Serve, D. W. Hobson, L. H. Lee and J. Uddin, *Toxicol. Environ. Health, Part A,* 1992, **37,** 313.

13 (a) S. L. Yost, J. C. Pennington, J. M. Brannon and C. A. Hayes, *Mar. Pollut. Bull.,* 2007, **54,** 1262-1266; (b) H. Muthurajan, R. Sivabalan, M. B. Talawar and S. N. Asthana, *J. Hazard. Mater.,* 2004, **112,** 17-33.

14 G. He, H. Peng, T. Liu, M. Yang, Y. Zhang and Y. Fang, *J. Mater. Chem.,* 2009, **19,** 7347-7353.

15 (a) S. Madhu, A. Bandela and M. Ravikanth, *RSC Adv.,* 2014, **4,** 7120-7123; (b) G. Sivaraman, B. Vidya and D. Chellappa, *RSC Adv.,* 2014, **4,** 30828-30831; (c) W. Xue, Y. Zhang, J. Duan, D. Liu, Y. Ma, N. Shi, S. Chen, L. Xie, Y. Qian and W. Huang, *J. Mater. Chem. C,* 2015, **3,** 8193-8199.

16 Y. Peng, A.-J. Zhang, M. Dong and Y.-W. Wang, *Chem. Commun.,* 2011, **47,** 4505-4507.

17 (a) H.-T. Feng and Y.-S. Zheng, *Chem. Eur. J.,* 2014, **20,** 195-201; (b) V. Bhalla A. Gupta, and M. Kumar, *Org. Lett.,* 2012, **14,** 3112-3115; (c) V. Bhalla, S. Pramanik and M. Kumar, *Chem. Commun.,* 2013,

49, 895-897; (d) V. Vij, V. Bhalla, and M. Kumar, *ACS Appl. Mater. Interfaces,* 2013, **5,** 5373-5380; (e) Y. Xu, B. Li, W. Li, J. Zhao, S. Sun and Y. Pang, *Chem. Commun.,* 2013, **49,** 4764-4766; (f) A. Ding, L. Yang, Y. Zhang, G. Zhang, L. Kong, X. Zhang, Y. Tian, X. Tao, and J. Yang, *Chem. Eur. J.,* 2014, **20,** 12215-12222; (g) P. B. Pati and S. S. Zade, *Tetrahedron Lett.,* 2014, **55,** 5290-5293; (h) K. Acharyya and P. S. Mukherjee, *Chem. Commun.,* 2014, **50,** 15788-15791; (i) R. Chopra, V. Bhalla, M. Kumar and S. Kaur, *RSC Adv.,* 2015, **5,** 24336-24341; (j) A. Chowdhury and P. S. Mukherjee, *J. Org. Chem.,* 2015, **80,** 4064-4075; (k) D. Samanta and P. S. Mukherjee , *Dalton Trans.,* 2013, **42,** 16784-16795; (l) S. Shanmugaraju, S. A. Joshi and P. S. Mukherjee, *J. Mater. Chem.,* 2011, **21,** 9130-9138; (m) B. Gole, S. Shanmugaraju, A. K. Bar and P. S. Mukherjee, *Chem. Commun.,* 2011, **47,** 10046-10048; (n) S. Shanmugaraju, H. Jadhav, R. Karthik and P. S. Mukherjee, *RSC Adv.,* 2013, **3,** 4940-4950; (o) B. Roy, A. K. Bar, B. Gole and P. S. Mukherjee, *J. Org. Chem.,* 2013, **78,** 1306-1310.

18 K. Tanaka, M. Murakami, J.-H. Jeon and Y. Chujo, *Org. Biomol. Chem.,* 2012, **10,** 90-95.

19 Gaussian 09, Revision A.02, M. J. Frisch, G. W. Trucks, H. B. Schlegel, G. E. Scuseria, M. A. Robb, J. R. Cheeseman, G. Scalmani, V. Barone, B. Mennucci, G. A. Petersson, H. Nakatsuji, M. Caricato, X. Li, H. P. Hratchian, A. F. Izmaylov, J. Bloino, G. Zheng, J. L. Sonnenberg, M. Hada, M. Ehara, K. Toyota, R. Fukuda, J. Hasegawa, M. Ishida, T. Nakajima, Y. Honda, O. Kitao, H. Nakai, T. Vreven, J. A. Montgomery, Jr., J. E. Peralta, F. Ogliaro, M. Bearpark, J. J. Heyd, E. Brothers, K. N. Kudin, V. N. Staroverov, R. Kobayashi, J. Normand, K. Raghavachari, A. Rendell, J. C. Burant, S. S. Iyengar, J. Tomasi, M. Cossi, N. Rega, J. M. Millam, M. Klene, J. E. Knox, J. B. Cross, V. Bakken, C. Adamo, J. Jaramillo, R. Gomperts, R. E. Stratmann, O. Yazyev, A. J. Austin, R. Cammi, C. Pomelli, J. W. Ochterski, R. L. Martin, K. Morokuma, V. G. Zakrzewski, G. A. Voth, P. Salvador, J. J. Dannenberg, S. Dapprich, A. D. Daniels, O. Farkas, J. B. Foresman, J. V. Ortiz, J. Cioslowski, and D. J. Fox, Gaussian, Inc., Wallingford CT, 2009.

20 A. D. Becke, *Phys. Rev. A,* 1988, **38,** 3098.

21 C. Lee, W. Yang and R. G. Parr, *Phys. Rev. B,* 1988, **37,** 785.

22 (a) S. S. Nagarkar, A. V. Desai and S. K. Ghosh, *Chem. Commun.,* 2014, **50,** 8915-8918; (b) W. Wu, S. Ye, G. Yu, Y. Liu, J. Qin and Z. Li, *Macromol. Rapid Commun.,* 2012, **33,** 164-171.

23 D. Zhao and T. M. Swager, *Macromolecules,* 2005, **38,** 9377-9384; (b) J. Liu, Y. Zhong, P. Lu, Y. Hong, J. W. Y. Lam, M. Faisal, Y. Yu, K. S. Wong and B. Z. Tang, *Polym. Chem.,* 2010, **1,** 426-429; (c) H. Arora, V. Bhalla and M. Kumar, *RSC Adv.,* 2015, **5,** 32637–32642.

24 (a) V. Bhalla, A. Gupta, M. Kumar, D. S. S. Rao and S. K. Prasad, *ACS Appl. Mater. Interfaces,* 2013, **5,** 672-679; (b) S. Pramanik, V. Bhalla, M. Kumar, *Anal. Chim. Acta,* 2013, **793,** 99-106; (c) L. Ding, Y. Bai, Y. Cao, G. Ren, G. J. Blanchard and Y. Fang, *Langmuir,* 2014, **30,** 7645-7653.

25 (a) P. Vishnoi, S. Sen, G. N. Patwari and R. Murugavel, *New J. Chem.*, 2015, 39, 886-892; (b) S. J. Toal and W. C. Trogler, *J. Mater. Chem.,* 2006, **16,** 2871-2883; (c) J. C. Sanchez, A. G. DiPasquale, A. L. Rheingold and W. C. Trogler, *Chem. Mater.,* 2007, **19,** 6459-6470.

26 (a) J. Wang, J. Mei, W. Yuan, P. Lu, A. Qin, J. Sun, Y. Ma and B. Z. Tang, *J. Mater. Chem.,* 2011, **21,** 4056-4059; (b) W. Wei, X. Huang, K. Chen, Y. Tao and X. Tang, *RSC Adv.,* 2012, **2,** 3765-3771; (c) S. Ramachandra, Z. D. Popovic, K. S. Schuermann, F. Cucinotta, G. Calzaferri and L. D. Cola, *Small,* 2011, **7,** 1488-1494.

27 (a) C. A. Anderson, P. G. Taylor, M. A. Zeller and S. C. Zimmerman, *J. Org. Chem.,* 2010, **75,** 4848－4851; (b) L. Váradi, M. Gray, P. W. Groundwater, A. J. Hall, A. L. James, S. Orenga, J. D. Perryd and R. J. Anderson, *Org. Biomol. Chem.,* 2012, **10,** 2578-2589; (c) C. Alvarez-Rua, S. García-Granda, S. Goswami, R. Mukherjee, S. Dey, R. M. Claramunt, M. D. S. María, I. Rozas, N. Jagerovic, I. Alkortae and J. Elguero, *New. J. Chem.,* 2004, **28,** 700-707; (d) S. Goswami, R. Mukherjee, R. Mukherjee, S. Jana, A. C. Maity and A. K. Adak, *Molecules,* 2005, **10,** 929-936; (e) S. Dey, D. Saina and S. Goswami, *RSC Adv.,* 2014, **4,** 428-433.

1,8-Naphthyridine-based fluorescent receptors for picric acid detection in aqueous media

Mandeep K. Chahal and Muniappan Sankar*
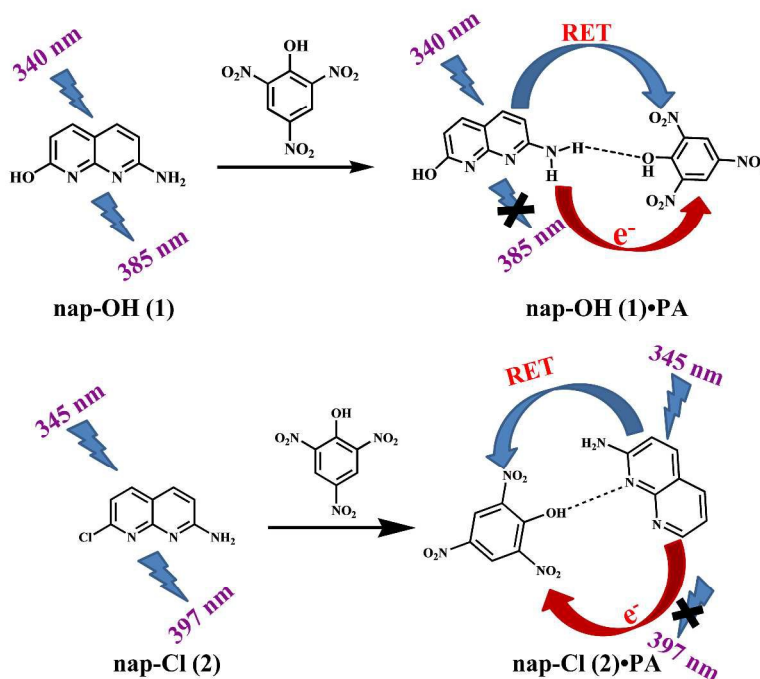
Naphthyridinic fluorescent receptors (**1** and **2**) were utilized for the selective detection picric acid (PA) in aqueous media which are able to detect ~ 1 ppm of PA *via* fluorescent 'turn off' mode.